EUROPEAN ORGANIZATION FOR NUCLEAR RESEARCH
European Laboratory for Particle Physics

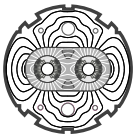

Large Hadron Collider Project

LHC Project Report 96–87

LHC BEAM DUMP DESIGN STUDY

Part II : Thermal analysis; implications for abort repetition and cooling system

S. Péraire and J.M. Zazula

Abstract

This second part of the LHC beam dump design study is devoted to transient and steady state nonlinear heat transfer analysis. Heat generation loads are imported from Part I: simulation of energy deposition in the graphite by particle cascades induced by the LHC primary protons, and superposition of identical energy distribution from each bunch along positions defined by the beam sweep profile on the upstream face of the core. A parametric finite element model of the dump including graphite core, aluminium frame, base plate with cooling channels, and shielding blocks, is elaborated and resolved by means of the ANSYS Engineering System, providing the transient evolution of internal temperature fields. Steady state analysis is then performed, by means of numerical approximations using a limited number of ANSYS results as an interpolation – extrapolation base. Only periodic aborts are considered. The first conclusion is that the dump requires several hours of cooling after each beam abort. Influence of natural cooling and thermal contact, and performance of a proposed water cooling system, are considered for single and repetitive beam dumping. At the ultimate intensity of $4.8 \cdot 10^{14}$ protons per beam, the dump assembly needs necessarily to be cooled to permit abort cycles as short as 13 h. At the nominal intensity of $3 \cdot 10^{14}$ protons, periodic aborts once per 5 h can be achieved without cooling. At any intensity, however, water cooling reduces the safe abort period by at least a factor 2. A third part of this study will concern mechanical analyses leading to graphite material specification.

SL Division

Administrative Secretariat
LHC Division
CERN
CH-1211 Geneva 23
Switzerland

Geneva, 8 January 1997

Contents

List of Tables

List of Figures

1 Introduction

The design study of the LHC beam dump [1] was initiated in Part I [2], with Monte Carlo ($\mathcal{MC}$) simulation of energy deposition by particle cascades induced by 7 TeV primary protons in graphite. The results confirmed that the aborted beam should be diluted. An optimised sweep profile was proposed, reducing the maximum local instantaneous temperature in the graphite to a safe level of about 1800^{o}C , for beam absorption at the maximum design intensity of $4.8{\cdot}10^{14}$ protons. Energy distribution from diluted beam at ultimate conditions defined size and alignment of the dump core.

Design of the LHC beam dump entails a time-dependent nonlinear thermal analysis (transient and steady state), to estimate temperature distribution as a function of time after beam abort. Deposited energy density obtained and discussed in Part I, determines the physical state of the dump immediately after a single abort, and forms thermal load input for heat transfer calculation. Maxima occur only in very small volumes, and for short time intervals. Long transient state of heat transfer is due to the extremely different time scales and load conditions of the two main time steps of a beam energy dissipation cycle: the first very short ($\leq$ 0.1 ms) step of beam and cascade impact, and the subsequent quite long ($\geq$ few hours) cooling step. Nonlinearity is due to temperature-dependent thermal properties of the materials.

The dump facility must safely absorb up to 540 MJ of the primary energy, and extract this energy out of the system within a reasonable delay, to bring internal temperature conditions to an acceptable level for the next beam abort. The full thermal analysis cannot therefore be limited to only one cooling cycle, and minimum safe delays must be defined between subsequent aborts, with respect to beam energy and intensity.

General assumptions made for the thermal analysis are summarised in Section 2. Details of finite element ($\mathcal{FE}$) model and solution procedures using the ANSYS [3] Engineering system are given in Section 3. Results for a single beam abort and cool-down are the subject of Section 4. Spatial distribution and time evolution of temperature in the graphite core and aluminium frame are presented for different boundary conditions: effects of natural cooling, imperfect thermal contact, and performance of a water cooling system are discussed. An overall time-dependent balance of the thermal energy in the system is also considered. The last two Sections are devoted to repetitive beam dumping, with special emphasise on maximum safe frequency of periodic aborts.

2 General assumptions

Nominal and ultimate parameters of the dumped LHC beam assumed for this study are summarised in Table 1 of this report.

Assumptions about $\mathcal{FE}$analysis are described in the next Section.

As already discussed (see Part I, Section 10), current state of the art on thermal analysis is restricted to a deposited power density at which the temperature rise in the graphite remains below 5000^{o}C . This is provided for by a beam sweeping system at any designed energy and intensity. Above this limit, phase transitions, variations in material density and pressure, and hydro-dynamic modes of energy transfer, would have to be taken into account. Only a highly improbable incident of absorption of undiluted beam at highest energy and intensity, cannot be considered within the frame of models applied in this report.

3 Finite Element analysis

3.1 Thermal properties of the materials

Physical properties of graphite, aluminium and iron, at room temperature, are given in Table 2 as they are assumed for the calculations from Refs. [7, 8]. Specific heat and conductivity of graphite and aluminium, as a function of temperature, are plotted in Figure 1. Simulation of energy deposition was repeated with a more probable graphite density, 1.85 g/cm^3 (1.75 g/cm^3 was assumed in Part I).

3.2 Solid geometry model

The geometry model of the LHC beam dump considered in the thermal analysis, consists of the following components:

1. a parallelepipedic graphite core of dimensions determined in Part I;
2. an aluminium frame laterally surrounding the core block;
3. a water-cooled aluminium base plate;
4. radiation shielding made from recuperated iron ISR magnets [5, 6].

All these components are defined by symbolic parameters, in order to study their individual influence and for eventual design modifications. The actual values of the geometrical parameters are listed in Table 3. The downstream Al and Fe absorbers, intercepting no more than 1% of the total energy of the cascades and separated from the main core of the dump, are not included in this thermal analysis.

3.3 Finite element model

The finite element model is based on first-order thermal elements (with temperature as a single degree of freedom), from the ANSYS library: 4-node PLANE55 for surfaces, and 8-node SOLID70 for volumes. Firstly, the front face of the dump is meshed with the plane elements, and then expanded 3-dimensionally along the dump length. The first nodes in the graphite are selected at the hottest positions representing centres of 35 bunch trains (each of 81 bunches) on the sweep curve. These 35 key-points are read from an external data file, created from the optimised beam sweep profile BUCKET55 (see Figure 5a in Part I). Thus, the lateral mesh within the core block has to be irregular, and this procedure facilitates eventual mesh modification. With these preselected nodes, an automatic meshing procedure produces 230 surface elements, of lateral size about 3×3 cm. Finer spatial resolution at the central region of maximum heat generation cannot unfortunately be achieved, as the whole assembly has to be comprised of one model, the total number of elements being restricted by program memory. The quadrilateral mesh is applied for the frame, base plate and shielding. Divisions of 8 elements on each lateral side of the core and frame are expanded from the corners towards the mid-sides; 20 element divisions along beam axis are also expanded upstream, to concentrate mesh in regions of substantial variations in energy deposition. The circular shape of the cooling channels is replaced by equivalent square profiles, preserving the same contact surface area between aluminium and water. As coarse a mesh as possible is applied for the iron blocks, considered only as heat sinks; the spatial distribution of temperature in the shielding is not of special interest, since it changes very little. The ultimate 3-dimensional $\mathcal{FE}$ model, containing 8834 nodes and 7812 elements, is shown in Figures 2a-b.

3.4 Boundary conditions and thermal contact

Heat evacuation by a water cooling is modelled as a convection boundary condition of the cooling channel surfaces. The water convection coefficient is an adjustable parameter (see Sec-

tion 3.6), depending mostly on the water flow. Heat leakage to the environment (natural cooling by surrounding air) is modelled by thermal convection through external boundaries of the shielding blocks. The concrete floor is assumed to be thermally insulated.

An important modification of the ideal model is the incorporation of imperfect thermal contact. This concerns especially the surface between core frame and base plate (contact A), and the two surfaces (contact B), between aluminium frame and top shielding, and between base plate and bottom shielding. Since no special thermal contact elements are foreseen in the ANSYS library, a thin (1 mm) layer of flat thermal-brick elements is inserted between the surfaces assumed to be in bad contact. With a presumed fraction (50% in layer A, and 25% in the two layers B) these elements are then randomly attributed to a good conductor (aluminium), and the rest to a bad conductor (air). This random model approximates the real situation, where the exact location of a good or bad contact is very hard to control. Perfect contact is assumed only between the graphite and the aluminium frame. As no contact can be accepted, for practical reasons, between the aluminium frame and the side iron blocks, the latter are assumed to be completely insulated, and separated by 3 cm gaps (see Figure 2a), in practice filled with air. The lateral blocks therefore play only an illustrative role in the $\mathcal{FE}$model.

3.5 Heat generation loads

During 86 μs of beam impact, the dump core is subjected to internal heat generation by particle cascades induced in the graphite by primaries. Heat generation rate used in the thermal calculation is obtained by superposition of identical energy distribution from each bunch along positions defined by the sweep profile on the upstream face of the core. The interface program, which transfers energy from $\mathcal{MC}$scoring bins (cylindrical mesh defined by axis of a single bunch) to the ANSYS nodal loads, is described in Refs. [4, 2]. The deposited energy distribution is integrated over the beam interception time; therefore it must be normalised to the beam intensity and expressed per unit time, in units of power density. The energy immediately absorbed from the cascades by parts of the dump far from the beam (frame, base plate, and shield) can be neglected, because of very low spatial concentrations and volume integrals when compared to the energy deposited in the core (see Table 6 in Part I).

3.6 Time steps, solution options and post-processing

A uniform temperature of 20^{o}C is assumed for the initial state of the dump. The first 86 μs time step of the transient analysis is additionally divided to at least 5 time sub-steps, to cope with non-linear temperature rise versus absorbed heat. For subsequent steps of thermal evolution (heat dissipation by conduction and evacuation by cooling) the thermal loads are set to zero. At the second time step (up to 1 hour after abort), an automatic sub-step adjustment is activated, providing for results to be stored in time intervals increasing from milliseconds up to 10 minutes. At the third (cooling) time step, fixed sub-steps of 1 hour are applied.

All the solution runs are consequently performed with PCG solver and Newton-Raphson procedure, recommended for nonlinear transient thermal problems. The ANSYS batch jobs are submitted to the ParC nodes of the SP-2 system at CERN. Basic results are nodal temperatures of all elements at the end of each time sub-step; output files (up to 50 Mb per run) are available for further interactive analysis. Control options for the solution and most of the post-processing procedures are programmed in the ANSYS system Parametric Design Language (APDL). Unfortunately, some useful ANSYS graphic options, *e.g.*, temperature colour contours animated in time,

cannot be reproduced in this report.

4 Single beam abort

All single beam abort calculations were performed at ultimate intensity.

4.1 Temperature distribution in graphite

Lateral temperature distribution, at depth of longitudinal maximum in the dump (z=220 cm), as it appears immediately after interception of a single swept beam, is shown in Figure 3a: the hottest area (white in the picture) indicates temperatures above 1000^{o}C . Graphic animation shows fast diffusion of the sharp isotherms initially resembling the BUCKET55 profile, as temperatures tend to equilibrate by heat dissipation. After 86 μs heating, maximum temperature in the graphite remains below 1200^{o}C , if averaged over elements of lateral size not smaller than 3 cm. Part I of this study [2] shows that this limit can be locally and momentary exceeded, in very small volumes: enthalpy calculation (see equation (1) in Part I) performed with a much finer lateral resolution of 1 mm^2 under the assumption of instantaneous heating, predicts local temperature in the graphite of up to 1800^{o}C , for the same sweep profile and beam intensity.

Maximum temperature in the graphite as a function of time is plotted in Figure 4a. Several seconds are required to cool the hottest region below 1000^{o}C . For so short a time, no cooling system is effective. After 1 h, some graphite zones still remain above 100^{o}C , in spite of good thermal contact with the aluminium frame and of external cooling system. More than 3 h of cooling in fact are necessary to bring the central temperature in the graphite below 50^{o}C .

However, initial temperature of the core edges (see Figure 4b) does not exceed 30^{o}C , due to a weak effect of direct energy absorption from the particle cascades (see also Section 8 of Part I). Thereafter, thermal conduction from the hot regions heats the edges of the block to above 130^{o}C , in about 20 minutes. The horizontal and longitudinal temperature profiles in the graphite are plotted in Figures 5a-b, at 86 μs, 6 or 24 mn, 1 h and 8 h after a single beam abort. After 6 mn, the maximum temperature drops to about 400^{o}C . After a little more than 1 h, the temperatures are below 100^{o}C , and could be considered as almost uniform. Thereafter, the cooling of the core is governed by the cooling of the aluminium frame.

4.2 Maximum temperature in aluminium frame

The internal surface temperature of the aluminium frame is taken to be identical to that on the external edges of the graphite block. For metallurgical reasons the temperature of the aluminium must be limited to 150^{o}C . A 3-dimensional part-section of the aluminium frame, with isotherms, is presented in Figure 3b. Since the external vertical sides are insulated thermally from the shielding (separated by air) and because of the specific sweep profile, the most critical temperature occurs at mid-height of the right edge. The maximum temperature is reached 15-25 mn after beam absorption; thereafter the temperature in the aluminium frame drops to a level that is evidently affected by the cooling conditions. Time evolution of maximum temperature in the aluminium, obtained from a single beam abort with different boundary conditions, is shown in Figures 6 and 7, and discussed in the following sections in the context of natural and water cooling. Evolution of the aluminium temperature for repetitive beam aborts is the subject of Section 5 of this report.

4.3 Effects of natural cooling and imperfect contact

Natural cooling of the dump core and frame is achieved by heat leakage to shielding blocks and surrounding air, but becomes effective only after a certain time. The two extreme cases from

test calculations of a single beam abort, presented in Figure 6 and in Table 4, concern the externally insulated frame, with no contact with base plate and shielding (labelled as M32 model), and the frame in perfect thermal contact with the external environment (M31 model). The latter model shows the aluminium temperature only 11^{o}C lower at the time of maximum (24 mn), but already 56^{o}C lower than M32 after 8 h. With no heat leakage to the environment (M32) the aluminium frame would still be above 90^{o}C after 8 h. A more realistic model (M36), with 50% contact through the base plate and 25% contact through the top and bottom shielding, provides maximum and final temperatures slightly higher than in the case of perfect contact (M31). The same tendency is maintained if heat is removed from the base plate by water cooling; in that case perfect contact with shielding (M30) lowers the temperature by 9^{o}C after 24 mn, and only by 2^{o}C after 8 h, respectively to the equivalent water-cooled model with no contact with the shield (M34). For the equivalent contact models with water cooling turned off/on (*e.g.*, M31 / M30 with perfect contacts, or more realistic M36 / M35), the presence of water cooling still cannot reduce the aluminium temperature at the time maximum, and only 6–7^{o}C can be achieved after 8 h. However, the following sections show that incorporation of water cooling is essential in preparing conditions for repetitive beam aborts.

4.4 Performance of the water cooling system

Heat flow rate extracted by a cooling system is proportional to the area in contact with the coolant, to the temperature gradient between the cooled material and the coolant, and to the thermal convection coefficient. The latter depends on the speed of the fluid and on several of its physical properties (density, specific heat, thermal conductivity, viscosity), as well as on diameter of the cooling channels. Classical hydraulic calculation shows that for water flow in pipes of diameter between 1 and 5 cm, with velocity between 0.5 and 13 m/s, the convection coefficient can vary between 0.2–3.6 $\cdot 10^4$ W$\cdot$m$^{-2}\cdot$K^{-1}. However, even if higher convection coefficient could be achieved, no significant gain in cooling efficiency (measured by reduction of maximum temperature in Al frame) can be expected for the convection coefficient of much higher order of magnitude than 10^4 W$\cdot$m$^{-2}\cdot$K^{-1}, for 2 cm diameter pipe. This is demonstrated by test calculation, summarised in Figure 7 and Table 5, where the convection coefficient, taken as parameter, is varied by 0.01 to 100 times the basic value. An explanation is provided by the saturation phenomenon: with more intense cooling, the temperature gradient on the contact surface between aluminium and water becomes smaller, which in turn reduces the heat flow rate. Moreover, the temperature criterion for aluminium concerns the spatial maximum (*i.e.*, the right edge of the frame) which is situated quite far away from the cooling channels. The required temperature gradient can be eventually increased by lowering the coolant temperature; however, the calculation with cooling water at 10^{o}C shows that only 4^{o}C can be gained in the aluminium temperature after 8 h, compared to cooling with water at 20^{o}C . Another possibility for improving the cooling performance could be an increased cooled surface area. However, calculation shows (see Table 5) that doubling the diameter of the 8 cooling channels (from 2 to 4 cm) gives only a negligible improvement, in the hottest zone of the Al; again, saturation may be the cause.

Almost all the cooling calculations of this report were made with water convection coefficient of 10^4 W$\cdot$m$^{-2}\cdot$K^{-1} and channel diameter of 2 cm, corresponding to 3.2 m/s water speed and 6400 Reynolds number. Finally, in order to reduce hydraulic erosion hazard, it was decided to drop the speed to 2 m/s, *i.e.*, 0.65$\cdot 10^4$ W$\cdot$m$^{-2}\cdot$K^{-1} convection coefficient and 3.2 cm diameter, for the same Reynolds number and the same cooling efficiency.

4.5 Time-dependent energy balance

Final evaluation of the cooling system might be based not only on the local criterion (*i.e.*, the temperature at a discrete point, at a certain time), but rather on the global (volume and time-integrated) criterion: the total thermal energy evacuated from the system over a long time interval. This can be estimated by the enthalpy reserve stored in different components of the dump, at different stages of at least one beam abort. Here, the enthalpy reserve in each material, as a function of time, is evaluated by temperature integration of the specific heat, from the initial temperature (20^{o}C) to the actual temperature averaged in each element, and then by integration over element volumes.

The aborted beam at maximum energy and intensity brings an energy of 540 MJ; out of this, only about 390 MJ is immediately (in 86 μs) absorbed in the core block, and converted into heat; shower simulation (Part I) shows that the rest escapes (downstream, or laterally) with the most penetrating cascade components. Time evolution of enthalpy in the graphite, aluminium and shielding iron, is shown in Figure 8a in the case of applied water cooling, and in Figure 8b in absence of it. Eight hours after the beam impact, the core block retains about 6% of the initial energy in the first case, and 10% in the second one. However, for the same 8 h interval, the water cooling system (as designed in M35 model, see Table 4) can evacuate about 35% of the initial thermal energy; about 50% goes to the shielding and only 8% remains in the aluminium frame. If no water cooling is applied (M36 model), the total energy evacuated in 8 h (by air convection only) is still negligible; about 72% heats up the shielding and 12% remains in the aluminium frame.

5 Repetitive beam aborts

Any simulation of heat transfer requires specification of initial conditions. Except prior to the first beam abort when a uniform room temperature is assumed, the initial temperature is rather hard to determine, since it is affected by the previous thermal history of the system. Moreover, at any point of a thermal field, temperature rise from repetitive heat input does not simply sum, but is rather dependent on the actual distribution of thermal gradients in the whole system and on boundary conditions; variation of material properties with temperature complicate even more this situation.

In practice, the dump facility needs to be prepared for beam abort at any phase of the LHC operation, with no a priori constant frequency. Such an irregular process would eventually require a statistical analysis, based on random sampling of energy and intensity of each aborted beam, which is not appropriate at the first stage of this study. Regular thermal cycles at least enable the estimation of a safe minimum dump cooling period, as a function of beam energy and intensity; this assumption is sufficient to evaluate the necessity and efficiency of a cooling system.

The evolution of maximum temperature during periodic series of 6 cycles of beam aborts is shown in Figures 9a-b-c-d for the graphite, and in Figures 10a-b-c-d for the aluminium frame, for periods of 1, 3, 6 and 8 h respectively. Figures 9a-b and 10a-b compare nominal and ultimate beam intensity, with and without water cooling. Figures 9c and 10c compare water cooling at ultimate intensity to no water cooling at nominal intensity. Figures 9d and 10d compare perfect to imperfect thermal contact, with water cooling at ultimate intensity.

The numerical results for the maximum and final temperatures in the graphite core and aluminium frame in the last of 6 successive beam abort cycles, are summarised in Table 6, for various cycle durations, beam intensities and cooling conditions. Several conclusions can be drawn:

– at ultimate intensity, water cooling is indispensable if the aluminium temperature is not to exceed

150^{o}C , for any abort repetition period up to 8 h;

– at nominal intensity, beam can seemingly be dumped without cooling for periods longer than 3 h (in fact longer than 5 h, see Subsection 6.3);
– no practical cooling system can prepare the dump to intercept multiple aborts of the 7 TeV beam at ultimate or nominal intensity, as frequently as once per hour;
– after 6 cycles, the thermal steady state is almost reached in graphite, even for (realistic) short periods; in the aluminium frame, thermal stability appears for none of the presented cases, even for period of 8 hours.

As maximum steady state temperature in the graphite remains well below the design constraint of 2500^{o}C , and as graphite cooling soon becomes governed by the aluminium frame cooling, the thermal stability discussed in the next Section is restricted to the aluminium frame.

6 Thermal stability in aluminium frame

Computation time is one of the most critical limitation for extensive ANSYS calculations: the time scale is 1 hour for a single beam abort and 10 hours for several thermal cycles. Therefore, it is difficult to perform a single abort cooling analysis up to a quasi-asymptotic temperature (see Subsection 6.1 below), and almost impossible to perform thermal cycling up to an evident steady state (see 6.3). It is worth noting that the static thermal analysis available in ANSYS (time-constant loads) is of no help here, because of the extremely high heating/cooling time ratio.

Numerical approximations then become attractive, using a limited number of ANSYS results as an interpolation-extrapolation base, without any physical assumptions or with very simple ones. These, even of fair absolute value accuracy, are of an obvious comparative interest.

6.1 Quasi-asymptotic temperature of single abort

After about 2 hours, the cooling plots shown in Figure 6 for instance, seem to fit an exponential decrease. As a mater of fact, it is almost always possible to match the last part of any of these curves (starting from t_o), to a function of the form:

$$T(t) = (T_o - T_{as}) \cdot \exp\left(\frac{t_o - t}{\tau}\right) + T_{as} \qquad (t << \infty) \tag{1}$$

(t_o, T_o) and (t, T) being the starting and current coordinates, τ a time constant, and T_{as} the asymptotic temperature. This latter should not be considered as the temperature after an infinite cooling (which is obviously ambient temperature), but as a quasi-asymptotic temperature reached at the stage of lower water cooling performance, when the aluminium cooling (frame and plate) is governed by heat extraction to the shielding. Table 4 gives these asymptotic temperatures for the plots shown in Figure 6.

6.2 Extreme temperatures of periodic aborts

Thermal cycling of different period (1 to 8 hours), different number of cycles (no more than 6, for computation time limitation), different boundary conditions (cooling, contact) and different beam intensity, have been studied; some of these are summarised in Table 6. Extreme temperatures for each cycle of periodic beam aborts are of special interest; under identical boundary and intensity conditions, these extrema can be interpolated between 1 hour and ∞, as functions of the period (p):

$$T_{Max}(i,p) = a(i) + \frac{b(i)}{p} + \frac{c(i)}{p^2} \tag{2a}$$

$$T_{min}(i,p) = f(i) + \frac{g(i)}{p} + \frac{h(i)}{p^2} \tag{2b}$$

i being the cycle index (from 1 to 6); the coefficients a, b, c, f, g and h resulting, for each cycle i, from a $1/p$ parabolic fit through the ANSYS basic results (for $p = \infty$, 6, 3 and 1 hour for instance). $T_{Max}(1,p)$ is assumed to depend only on the intensity, and $T_{min}(1,p)$ to be ambient temperature. Figures 12a-b present T_{Max} and T_{min} in the aluminium frame, as functions of dumping frequency ($1/p$): 12-a for water cooling at ultimate intensity, 12-b without water cooling at nominal intensity, both with imperfect contacts.

6.3 Steady state

Figures 10 suggest that after several cycles, each of extreme temperatures practically equalise; their asymptotic value defines the steady state level.

Both T_{Max} and T_{min} being defined for any realistic period p, from the first cycle to the 6-th, exponential extrapolation may again be performed, starting, *e.g.*, from the 4-th cycle:

$$T_{Max}(j,p) = [T_{Max}(4,p) - T_{Max}(\infty,p)] \cdot \exp\left(\frac{4-j}{\alpha_M}\right) + T_{Max}(\infty,p) \tag{3a}$$

$$T_{min}(j,p) = [T_{min}(4,p) - T_{min}(\infty,p)] \cdot \exp\left(\frac{4-j}{\alpha_m}\right) + T_{min}(\infty,p) \tag{3b}$$

j being the cycle index (from 4 to ∞), α a constant, $T_{Max}(\infty,p)$ and $T_{min}(\infty,p)$ the maximum and minimum steady state temperatures for beam aborts of period p, under specified intensity and boundary conditions (see Table 6). Successive j values of 5 and 6 in (3a) or (3b), produce a 2-equation system which determines the corresponding α and extremum. Figure 13 represents the maximum temperature T_{Max} in the aluminium frame, as a function of p, for nominal and ultimate intensity, with and without water cooling. In order not to exceed 150^{o}C , the period should be longer than 2.5 h at nominal intensity and longer than 12.5 h at ultimate intensity, with water cooling activated. Without it, these delays need to be multiplied by at least a factor 2, clearly demonstrating the necessity and efficiency of the water cooling system.

6.4 Beam intensity dependence

Almost all the ANSYS calculations assumed nominal or ultimate intensity. It is tempting to perform a linear interpolation of T_{Max} and T_{min} between these two limits, or better, a parabolic fit through ultimate, nominal and zero intensity. The extreme steady state temperatures can then be extrapolated as previously described. As an example, Figure 11 plots the first 6 cycles of ANSYS analysis of beam aborts of period 8 hours, at ultimate and $4{\cdot}10^{14}$ protons per beam intensities with imperfect thermal contact and no water cooling, and the corresponding approximated T_{Max} and T_{min} up to the steady state level. Comparison shows encouraging agreement between the numerical approximation and ANSYS solution; Figure 14 presents the minimum safe period (T_{Max}=150^{o}C in Al frame) of repetitive aborts, as a function of beam intensity, with and without water cooling. Again, at any intensity, the minimum abort period is at least 2 times longer in the absence of water cooling.

6.5 Irregular beam aborts

For safe beam dumping operation, precise rules of abort repetition will have to be laid down, taking into account variable energy, intensity and repetition. Some of the algorithms built to perform the numerical approximations presented in this Section could eventually be used; they are currently written in C-Nodal, but can easily be adapted to any other convenient control language.

Figure 14 shows that no abort repetition control is required up to $3.5 \cdot 10^{14}$ protons per beam, if the water cooling is activated, since the corresponding minimum safe period is below the minimum 4 h delay between two consecutive aborts. This is an argument for the implementation of the water cooling system even for low intensities.

7 Conclusions

The first conclusion of this report is that the LHC dump requires several hours of cooling time after each beam abort. Transient heat transfer analysis of single beam dumping at ultimate intensity, shows that more than 1 h of cooling is required to bring the maximum graphite temperature from an initial 1800^{o}C to below 100^{o}C ; temperature in the aluminium frame rises from an initial 30^{o}C to a maximum above 130^{o}C , in about 20 mn. Thereafter, the cooling of the core is governed by the cooling of the aluminium frame. This latter depends on the natural cooling conditions, on the thermal contacts between the various components of the dump assembly, and on an eventual forced cooling of the aluminium base plate. Natural cooling is achieved by ambient air convection, mainly acting on the surface of the shielding; its efficiency, although rather constant in time, is not sufficient. Thermal contact quality has very strong influence, but it is very hard to evaluate and improve. Finally, the best practical way to control the temperature is to implement a water cooling system in the aluminium base plate, as a compromise between technical, safety and economical considerations. The aim of such a system is to guarantee, under any conditions, 150^{o}C maximum temperature in the aluminium; maximum temperature in the graphite being, in any operational case, well below the design constraint of 2500^{o}C . Eight cooling channels of 3.2 cm diameter will provide a 1.6 l/s water flow at 2 m/s, along the 7 m length of the plate; increasing the water flow rate is unfortunately inefficient, because of saturation phenomenon.

In practice, the dump facility needs to be prepared for abort at any phase of the LHC operation, with no a priori constant frequency. Nevertheless, only periodic dumping is considered in this report, statistical analysis of irregular aborts being inappropriate at this stage of the study. Steady state analysis of the aluminium frame shows that the dump assembly needs necessarily be cooled at ultimate intensity, to enable periodic abort cycles as short as 13 h. At nominal intensity, periodic aborts once per 5 h can be achieved without cooling. At any intensity, however, water cooling reduces the safe abort period by at least a factor 2.

For safe beam dumping operation, precise rules of repetition will have to be laid down. Nevertheless, such a control is not required with water cooling, up to $3.5 \cdot 10^{14}$ protons per beam. This is an argument to implement it even for low intensities.

Acknowledgements

The authors of this note would like to thank E. Weisse for initiating and following up this work as the leader of the LHC Beam Dump Project. Special thanks are due to M. Ross for his indispensable support in writing this report.

References

[1] P. Lefèvre and T. Petterson (Eds.), "The Large Hadron Collider: Conceptual Design", CERN AC/95–05 (LHC), Geneva (October 1995).

[2] J.M. Zazula and S. Péraire, "LHC Beam Dump Design Study, Part I: Simulations of energy deposition by particle cascades; implications for the dump core and beam sweeping system", LHC Project Report 96–80, CERN, Genève (October 1996).

[3] Swanson Analysis Systems, *Inc.*, "ANSYS (Revision 5.2)", SASI/DN-P511:51, Houston, USA (Sept. 30, 1994).

[4] J.M. Zazula, "From particle cascade simulations (FLUKA) to finite element heat transfer and structural deformation analyses", presented at the *SARE'95 Workshop on Simulating Accelerator Radiation Environment*, CERN, Prévessin, France (October 9-11, 1995); CERN SL/95–93 (BT), Genève (October 1995).

[5] M. Ross, "ISR magnets for LHC dump shielding", CERN SL/BT memorandum (July 2, 1996).

[6] I. Dawson and G.R. Stevenson, "An Assessment of the Use of ISR Magnet-Yokes for the Shielding of the LHC Beam Dump", CERN/TIS–RP/IR/96-27, Genève (November 1996).

[7] G.W.C. Kaye and T.H. Laby, *"Tables of Physical and Chemical Constants"*, Longman Scientific & Technical, New York (1971).

[8] B.T. Kelly, *"Physics of graphite"*, Applied Science Publishers, LTD, London and New Jersey (1981).

Table 1: Ultimate and (nominal) parameters of the dumped LHC beam, assumed for this study.

Maximum proton momentum	7.0	TeV/c
Beam size (Gaussian σ_h=σ_v)	0.95	mm
Number of protons per bunch	1.70 (1.05)	$\cdot 10^{11}$
Number of bunches	2835	
Bunch duration	0.25	ns
Bunch spacing	25.0	ns
Beam intensity (protons)	4.8 (3.0)	$\cdot 10^{14}$
Stored beam energy	540 (333)	MJ
Overall beam abort time	86	μs
Minimum delay between 2 aborts	4	h
Typical delay between 2 aborts	12	h

Table 2: Physical properties of graphite, aluminium and iron, assumed in this report.

		Graphite (C)	Aluminium (Al)	Iron (Fe)
Density	[g·cm^{-3}]	**1.85**	2.70	7.88
Inelastic hadron interaction length	[cm]	37.3	35.4	15.1
Radiation length	[cm]	21.2	8.83	1.73
Specific heat (at 20^{o}C)	[J·g^{-1}·K^{-1}]	0.65	0.90	0.48
Thermal conductivity (at 20^{o}C)	[W·cm^{-1}·K^{-1}]	0.90	1.80	0.52
Maximum safe temperature	[^{o}C]	2500	150	
Melting (vaporisation) point	[^{o}C]	(5000)	660	1540

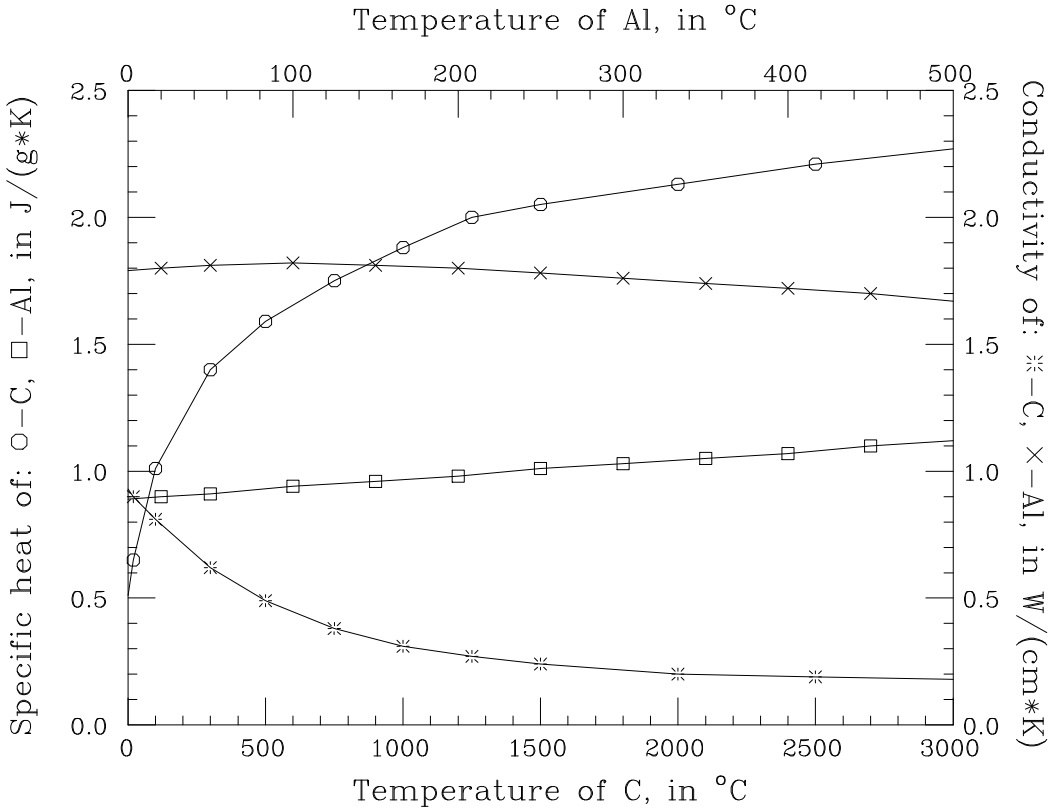

Figure 1: Thermal properties (specific heat and conductivity) of the graphite and aluminium, as a function of temperature, assumed for this study.

Table 3: Some important parameters of the finite element model of the LHC beam dump.

Dimensions of the graphite core	$70\times70\times700$	cm
(x, y) alignment of the core axis	(1,4)	cm
Thickness of the Al frame (base plate)	12 (16)	cm
Dimensions of a shielding block	$134\times110\times244$	cm
Thickness of imperfect contact layer	1	mm
No. and diameter of cooling channels	$8\times\oslash\,3.2$	cm
Convection coefficient of water	$0.65{\cdot}10^{4}$	$W{\cdot}m^{-2}{\cdot}K^{-1}$
Convection coefficient of ambient air	10	$W{\cdot}m^{-2}{\cdot}K^{-1}$
Cooling water (ambient air) temperature	20 (20)	^{o}C
Initial uniform temperature	20	^{o}C
No. of nodes along the sweep curve	35	
No. of nodes along core edges and depth	$8\times8\times20$	
Total number of nodes (elements)	8834 (7812)	
Minimum (maximum) time sub-step	$17{\cdot}10^{-6}$ (3600)	s

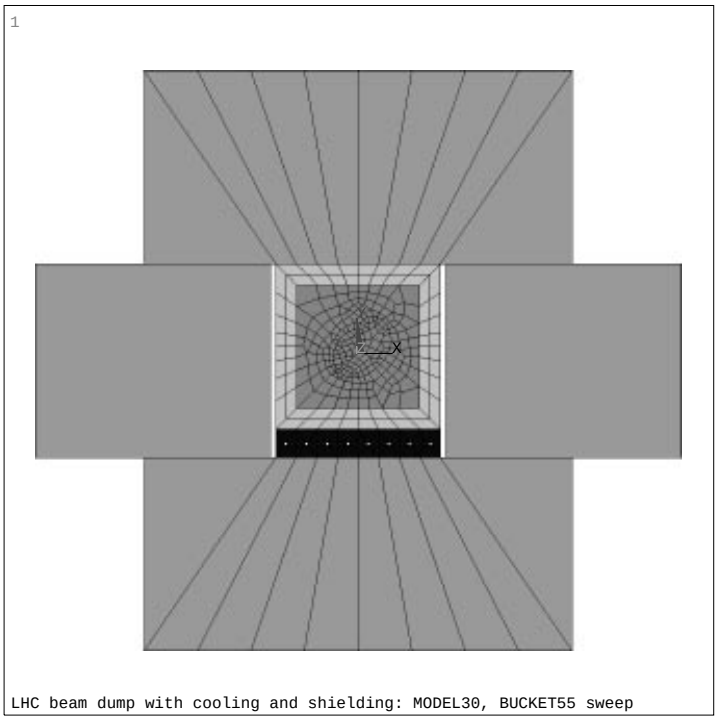

Figure 2a: Finite element model: lateral view of the upstream face of the graphite core, aluminium frame and iron shielding.

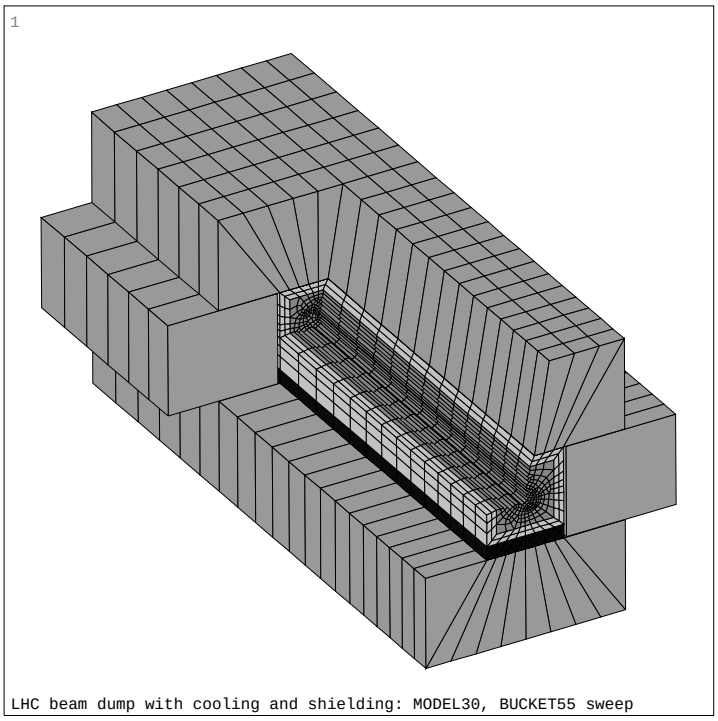

Figure 2b: Finite element model: part-section of the structure.

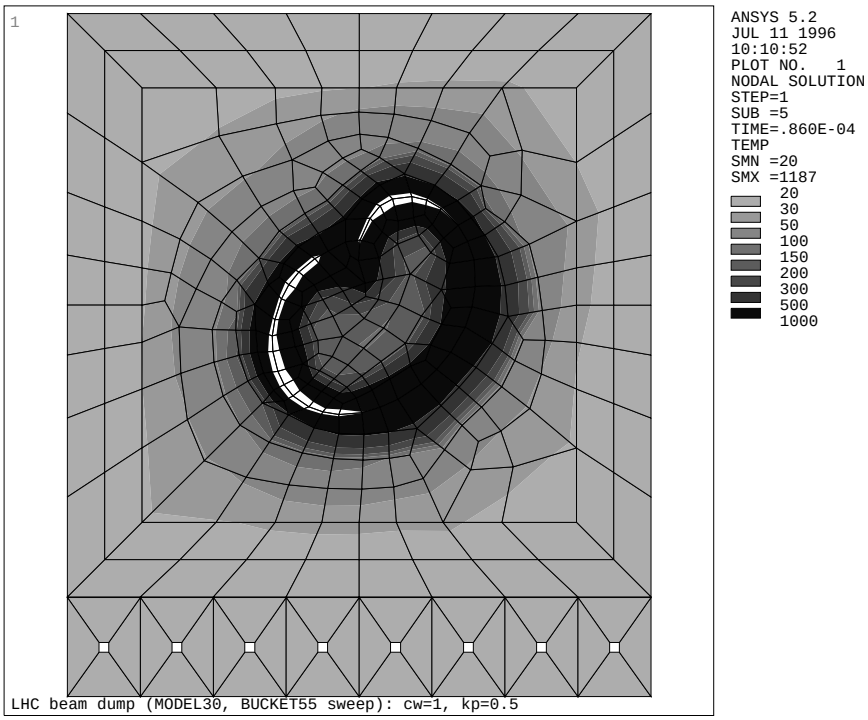

Figure 3a: Lateral temperature distribution at the longitudinal maximum, immediately after swept beam absorption at ultimate intensity.

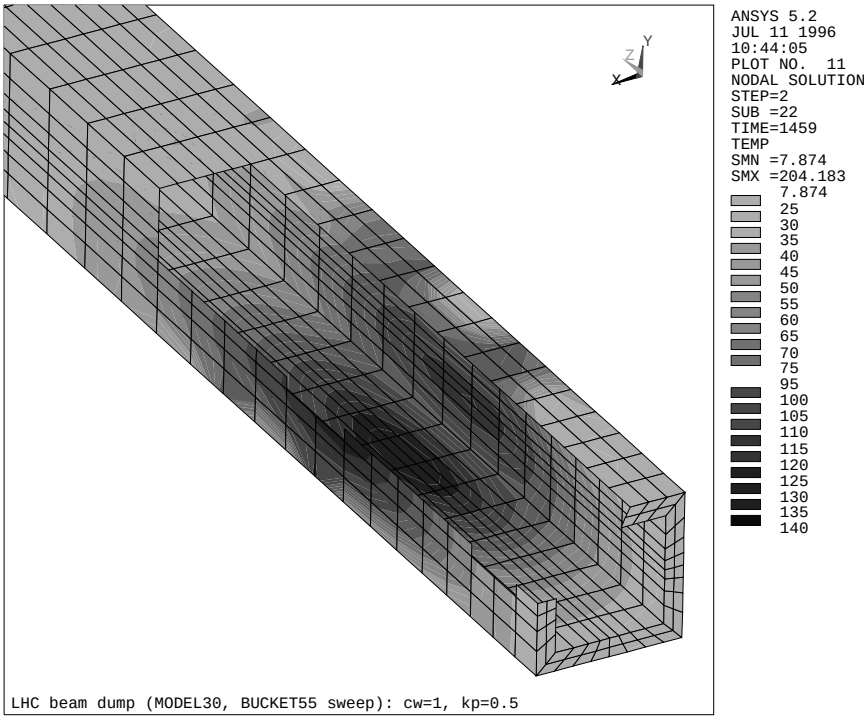

Figure 3b: Part-section of temperature distribution in the Al frame at the time of maximum (ultimate intensity).

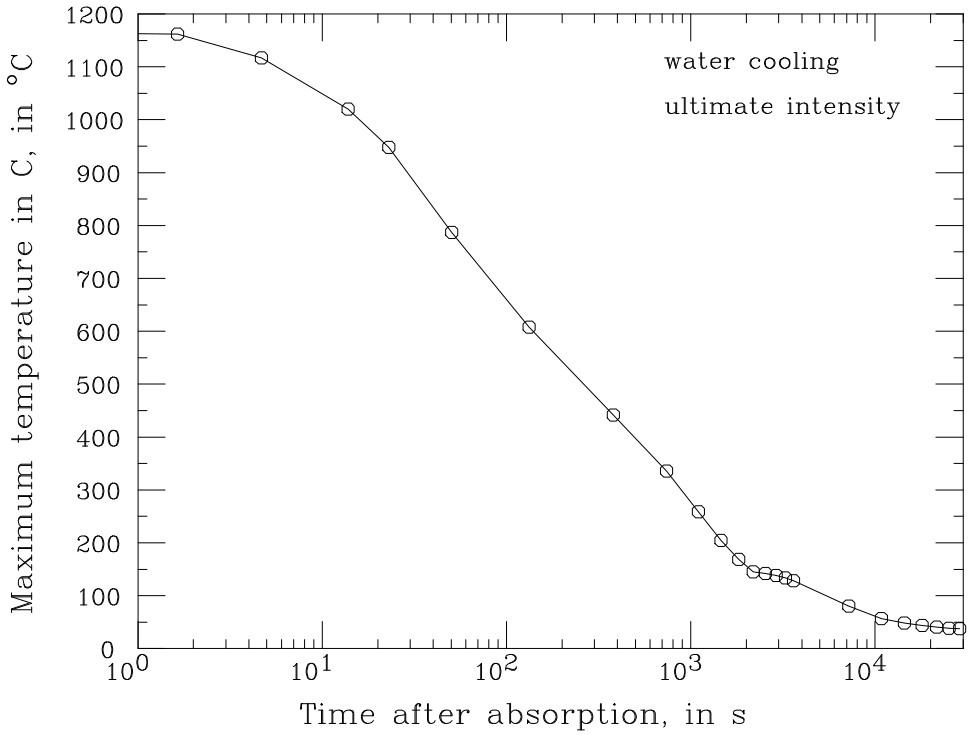

Figure 4a: Time evolution of maximum graphite temperature. Assumed conditions: BUCKET55 sweep, ultimate intensity, imperfect thermal contact, water cooling.

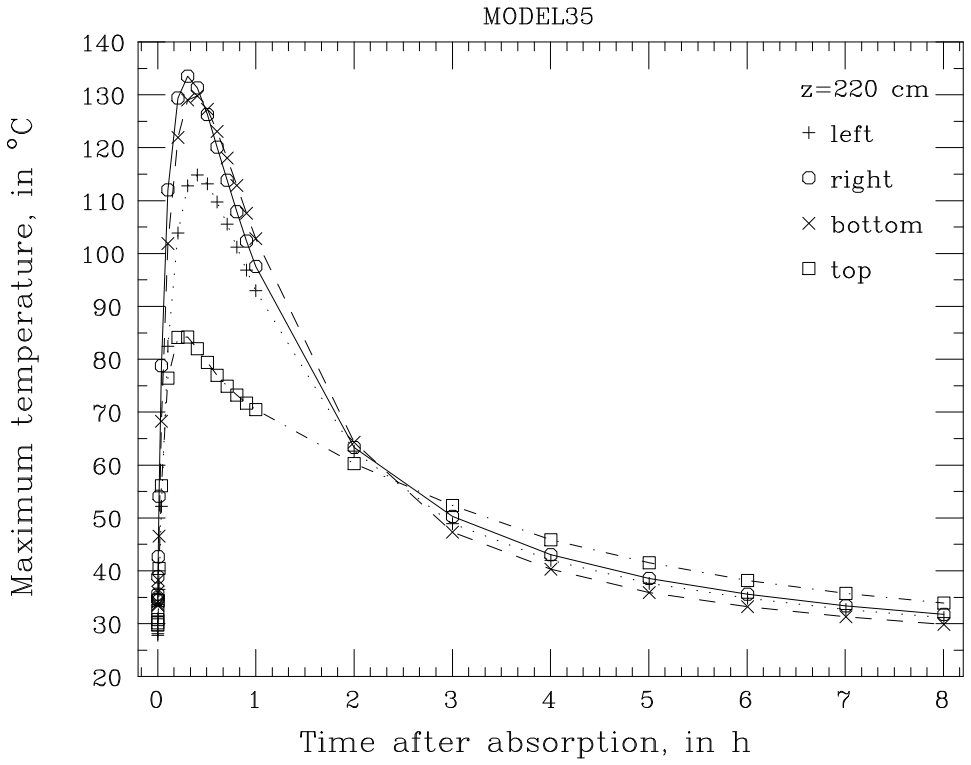

Figure 4b: Time evolution of the temperatures on the right, left, bottom and top edges of the graphite block, at depth of the longitudinal maximum (220 cm). Assumed conditions: BUCKET55 sweep, ultimate intensity, imperfect thermal contact, water cooling.

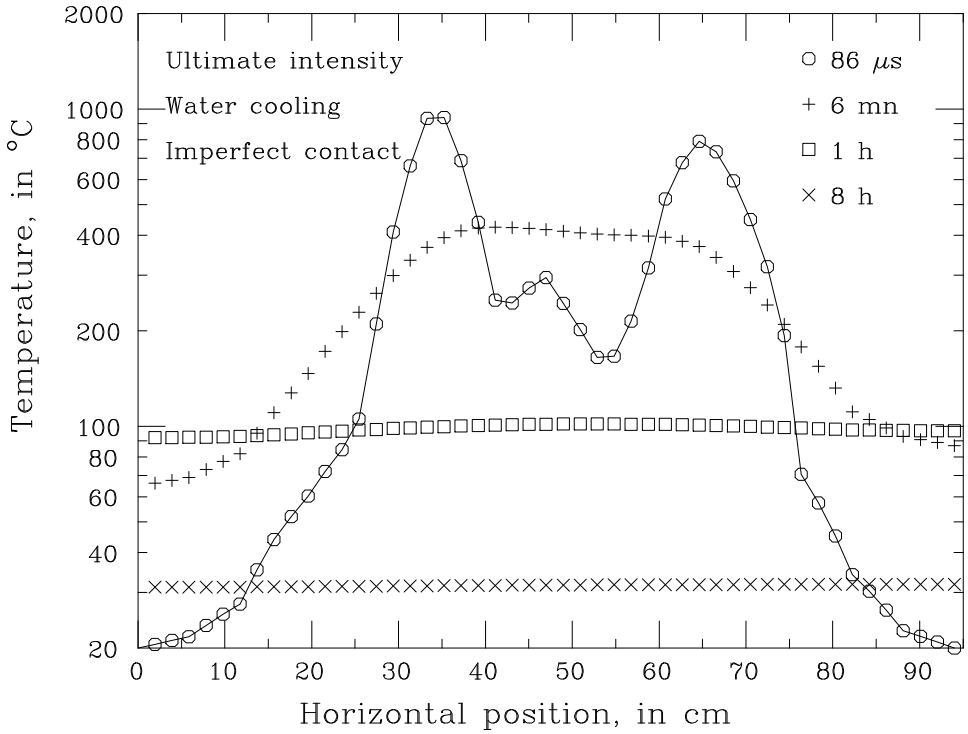

Figure 5a: Horizontal temperature profile at the longitudinal maximum (z=220 cm), at 4 different times after beam abort: 86 μs, 6 mn, 1 h and 8 h.

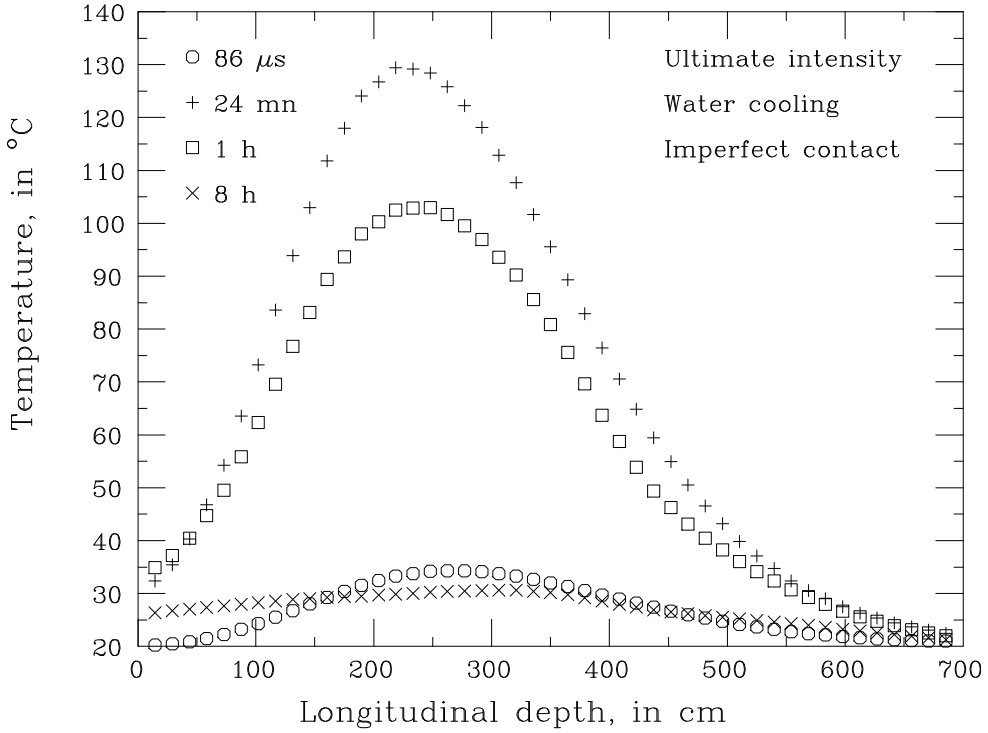

Figure 5b: Longitudinal temperature profile on the contact surface between graphite and Al at the top edge of the core, at 4 different times after beam abort: 86 μs, 24 mn, 1 h and 8 h.

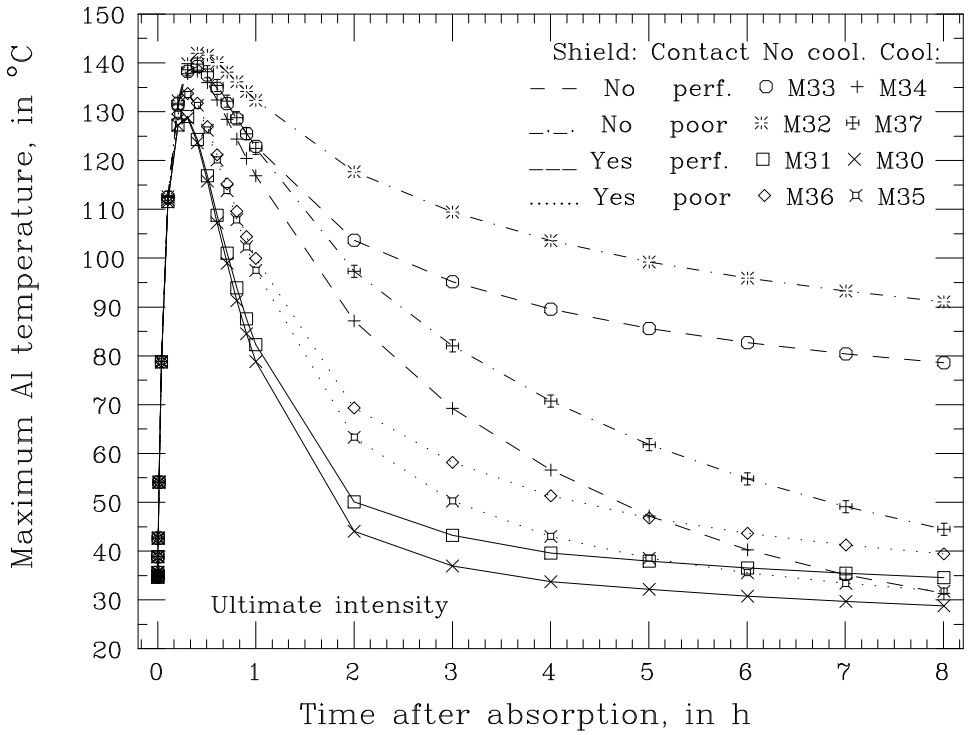

Figure 6: Time evolution of the maximum temperature in the Al frame, affected by thermal contact between different parts of the dump, and by water cooling. See the table below for explanation of the considered models.

Table 4: Maximum temperature in the Al frame, at the time maximum (T_{max}) and after 8 h of dump cooling (T_{8h}), affected by thermal contact between different parts of the dump, and by water cooling. Asymptotic temperature (T_{as}, see section 6.1) is also included.

Model	Thermal contact		Water	Al temperature [^{o}C]		
name	base plate	shielding	cooling	T_{max}	T_{8h}	T_{as}
M32	no	no	no	140	91	85
M33	100%	no	no	139	79	75
M34	100%	no	yes	138	31	21
M37	50%	no	yes	140	45	29
M31	100%	100%	no	129	35	34
M30	100%	100%	yes	129	29	28
M36	50%	25%	no	134	39	36
M35	50%	25%	yes	134	32	30

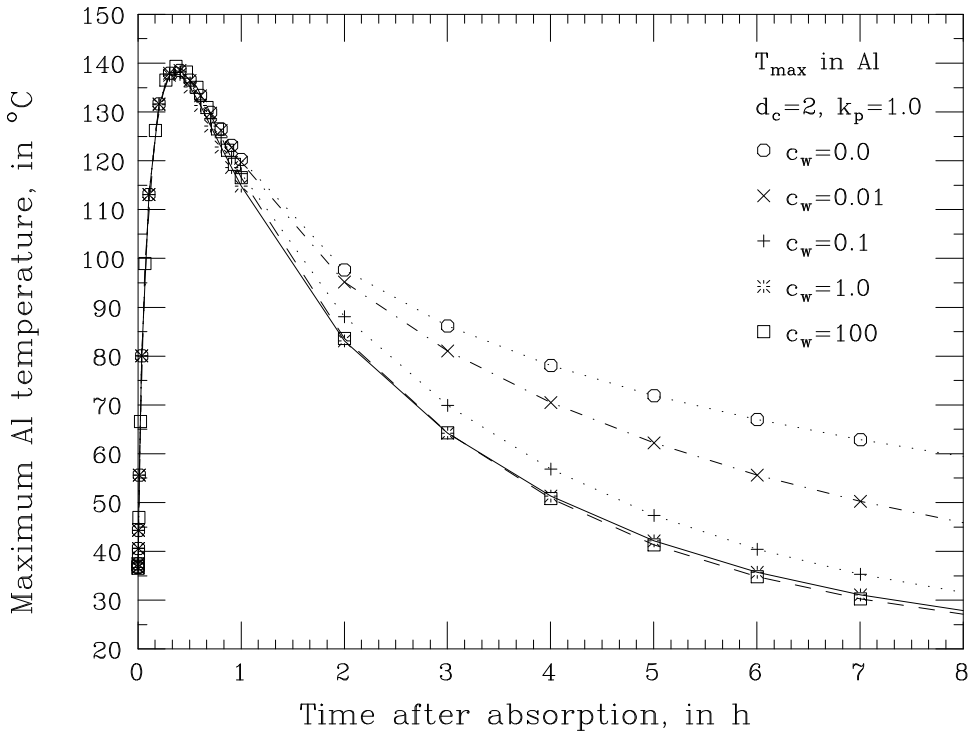

Figure 7: Time evolution of the maximum temperature in the Al frame, affected by convection coefficient of water cooling c_w (in 10^4 W·m^{-2}·K^{-1}). Assumed 2 cm diameter of the 8 cooling channels and perfect thermal contact between different parts of the dump.

Table 5: Influence of the cooling water convection coefficient c_w (in 10^4 W·m^{-2}·K^{-1}) and of the cooling pipe diameter d_c (in cm), on maximum temperature [^{o}C] in the Al frame at the time maximum (T_{max}), on temperature after 8 h of dump cooling (T_{8h}), and on final temperature of the cooling water (T_{wat}).

c_w	d_c	T_{max}	T_{8h}	T_{wat}
0	2.0	138.5	59.4	58.7
0.01	2.0	138.5	45.9	45.3
0.1	2.0	138.2	31.6	28.1
1	2.0	137.7	27.9	21.5
100	2.0	139.3	27.1	20.0
1	3.0	137.7	27.7	21.2
1	4.0	137.6	27.4	21.0

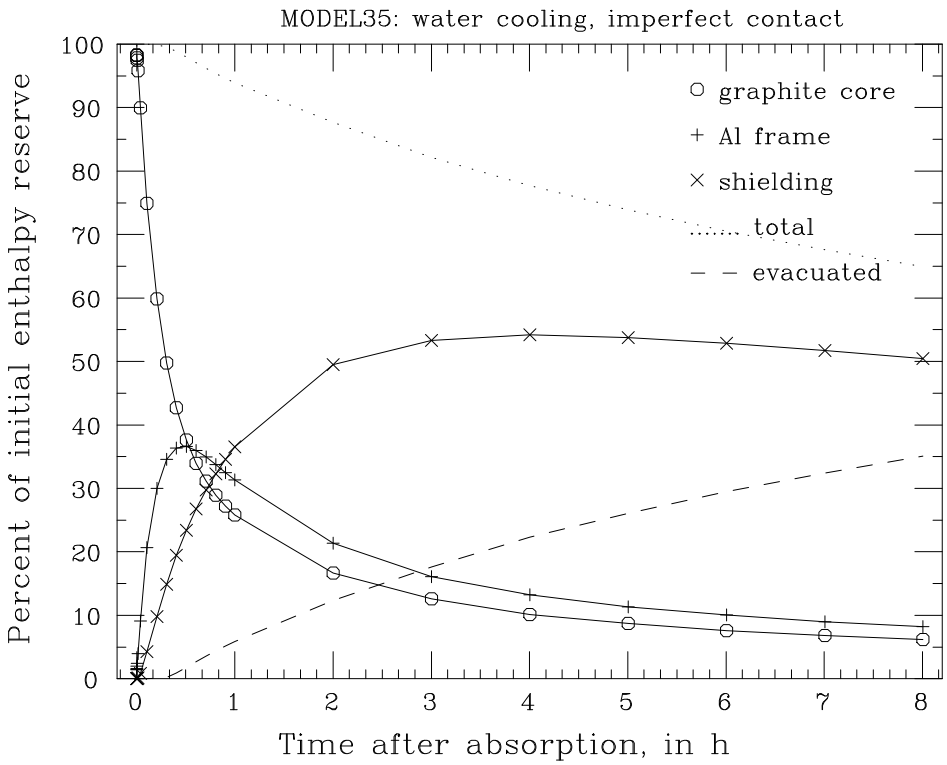

Figure 8a: Energy balance in various part of the dump, as a function of time, with water cooling.

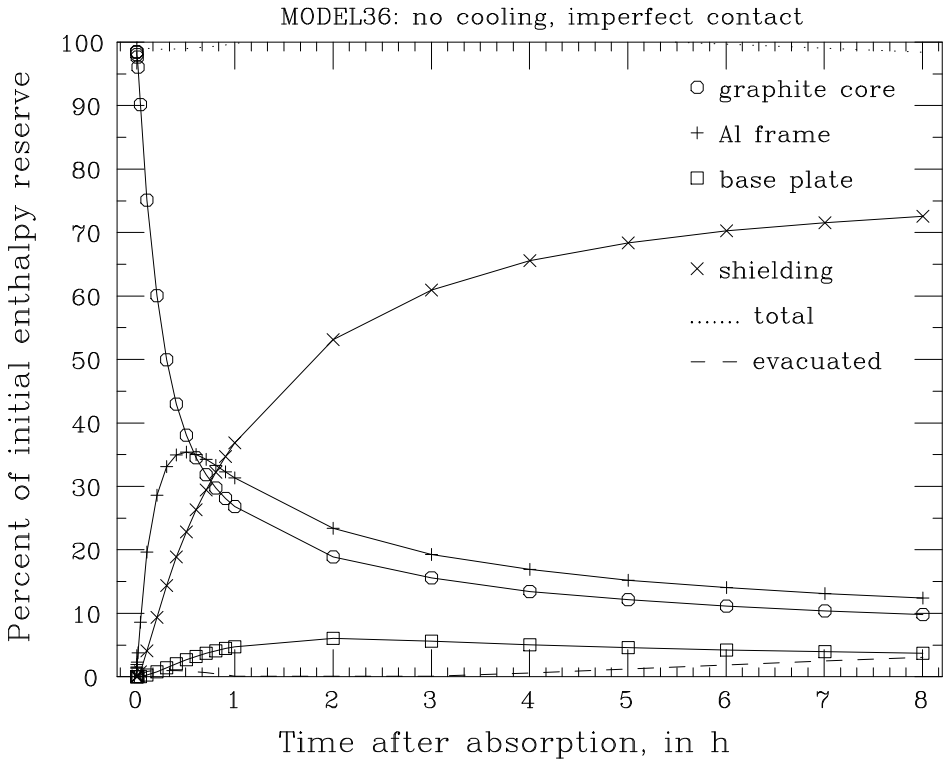

Figure 8b: Energy balance in various part of the dump, as a function of time, in absence of the cooling system.

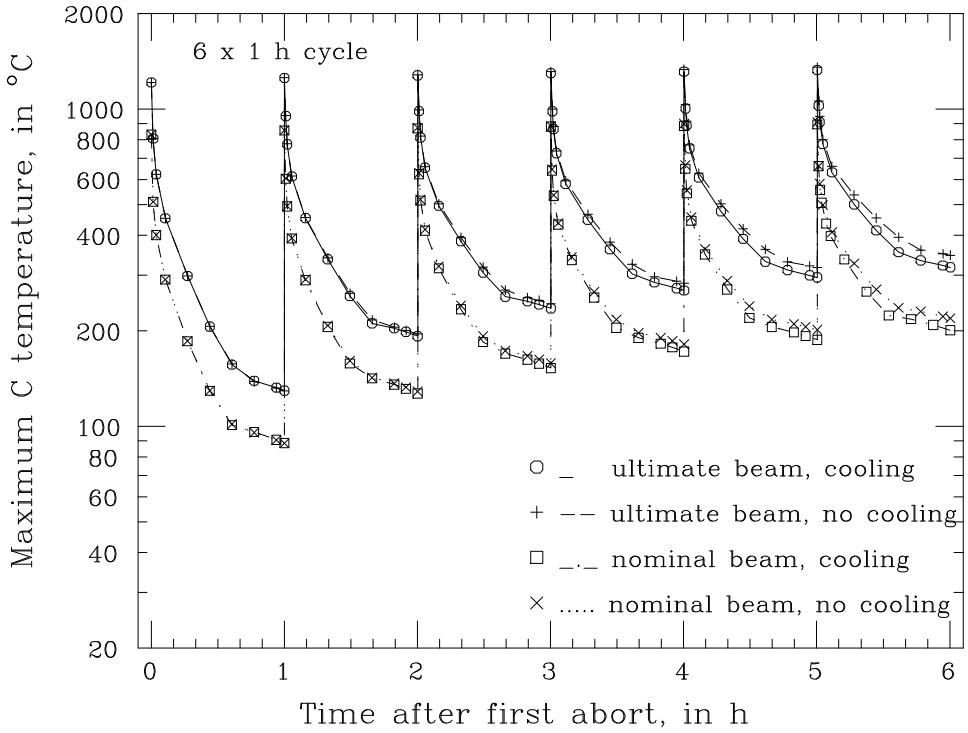

Figure 9a: Time evolution of the maximum temperature in the graphite, over the first 6 thermal cycles of 1 h, for nominal and ultimate beam intensity, with and without water cooling.

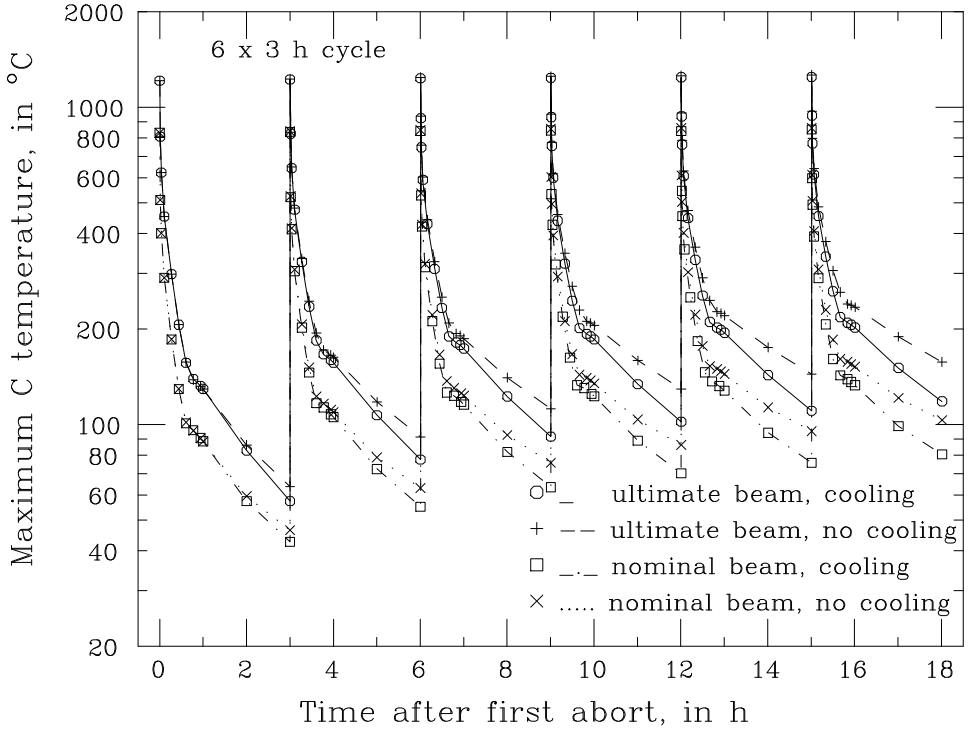

Figure 9b: Time evolution of the maximum temperature in the graphite, over the first 6 thermal cycles of 3 h, for nominal and ultimate beam intensity, with and without water cooling.

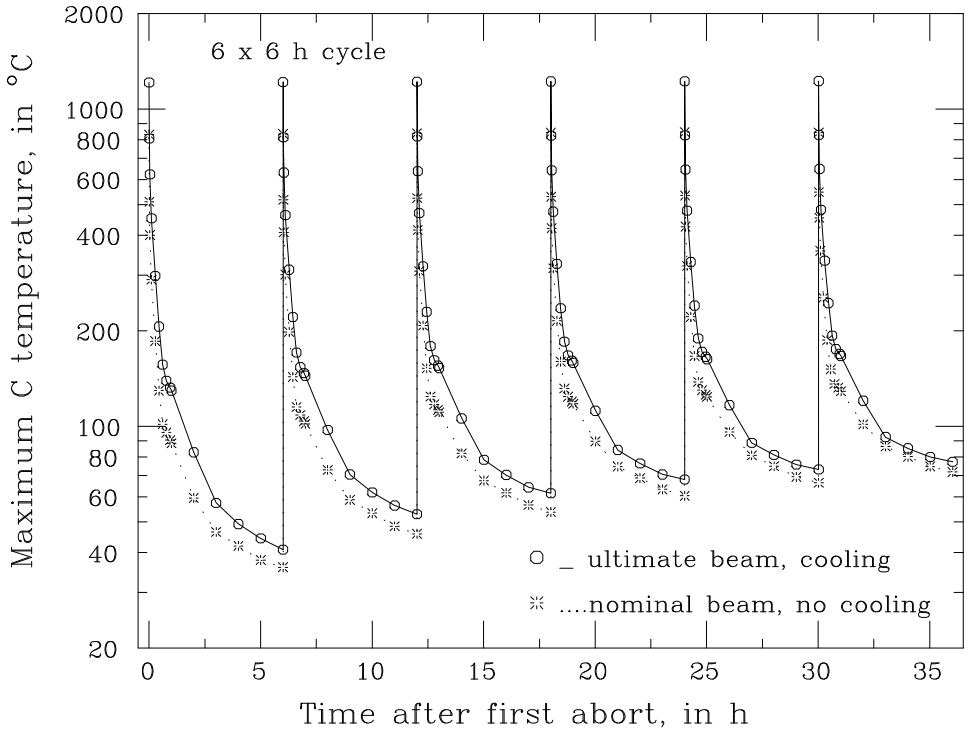

Figure 9c: Time evolution of the maximum temperature in the graphite, over the first 6 thermal cycles of 6 h, for nominal (no cooling) and ultimate (water cooling) beam intensity.

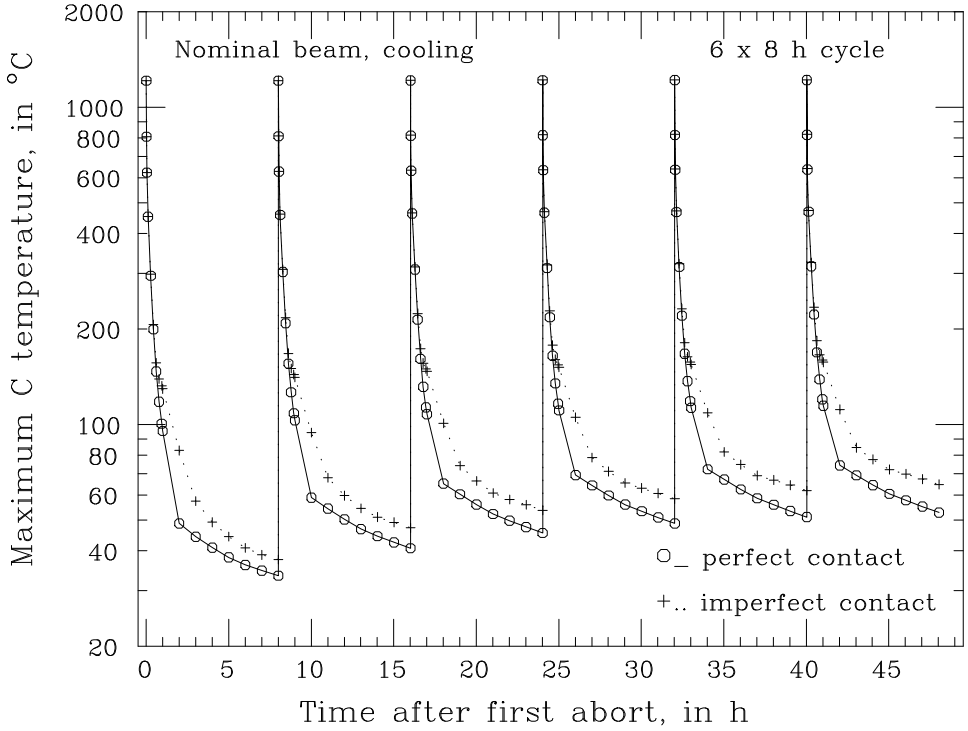

Figure 9d: Time evolution of the maximum temperature in the graphite, over the first 6 thermal cycles of 8 h, for perfect and imperfect contact (water cooling, ultimate intensity).

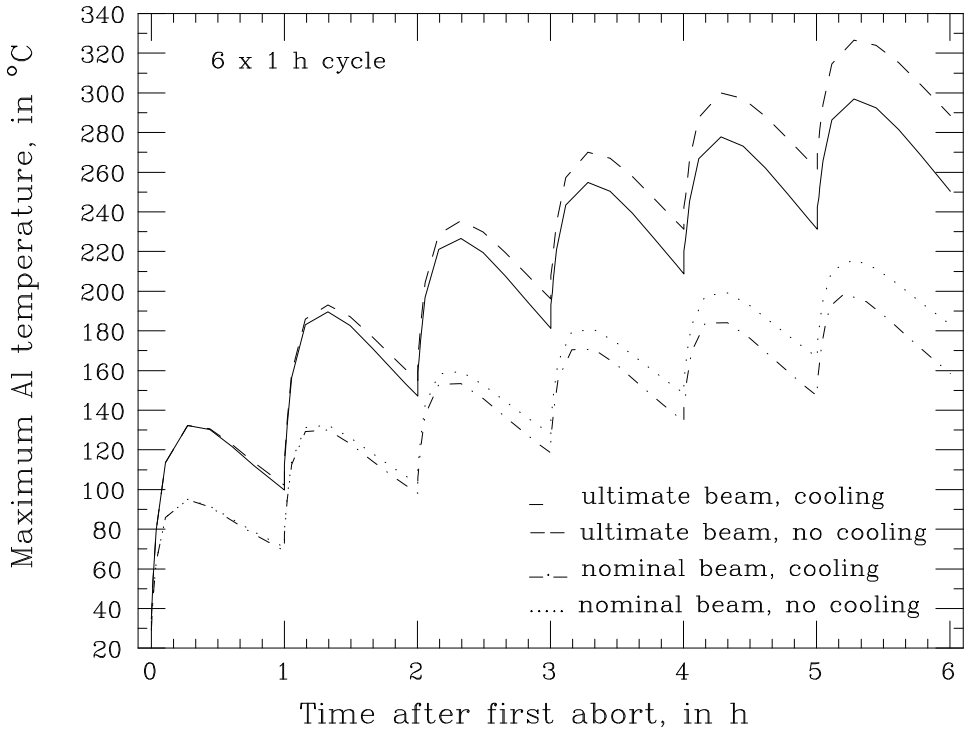

Figure 10a: Time evolution of the maximum temperature in the aluminium, over the first 6 thermal cycles of 1 h, for nominal and ultimate beam intensity, with and without water cooling.

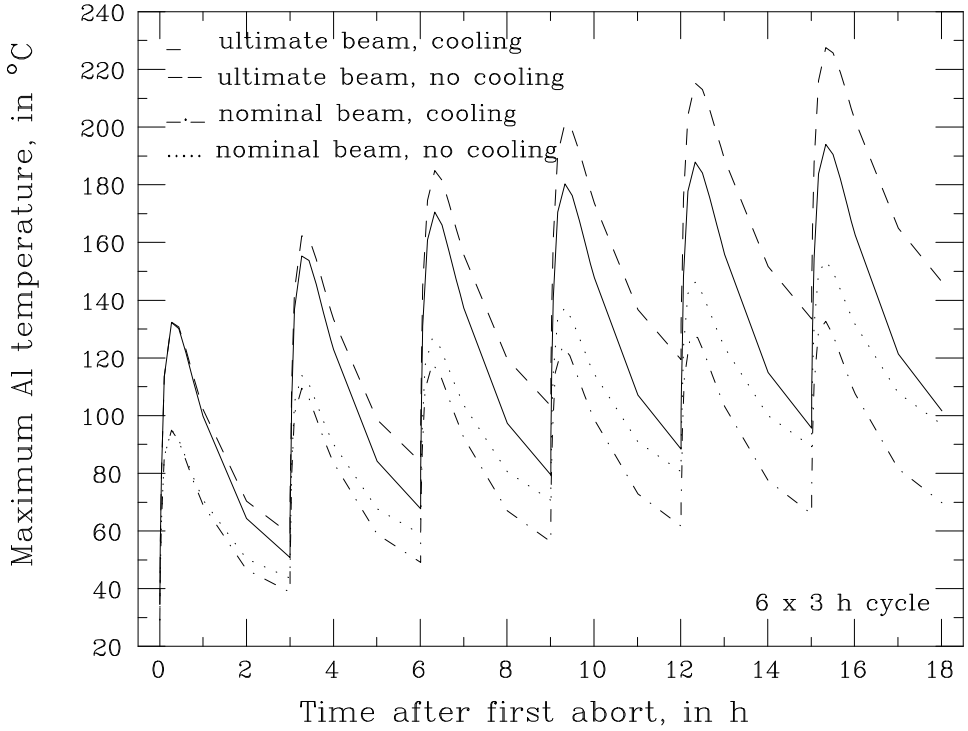

Figure 10b: Time evolution of the maximum temperature in the aluminium, over the first 6 thermal cycles of 3 h, for nominal and ultimate beam intensity, with and without water cooling.

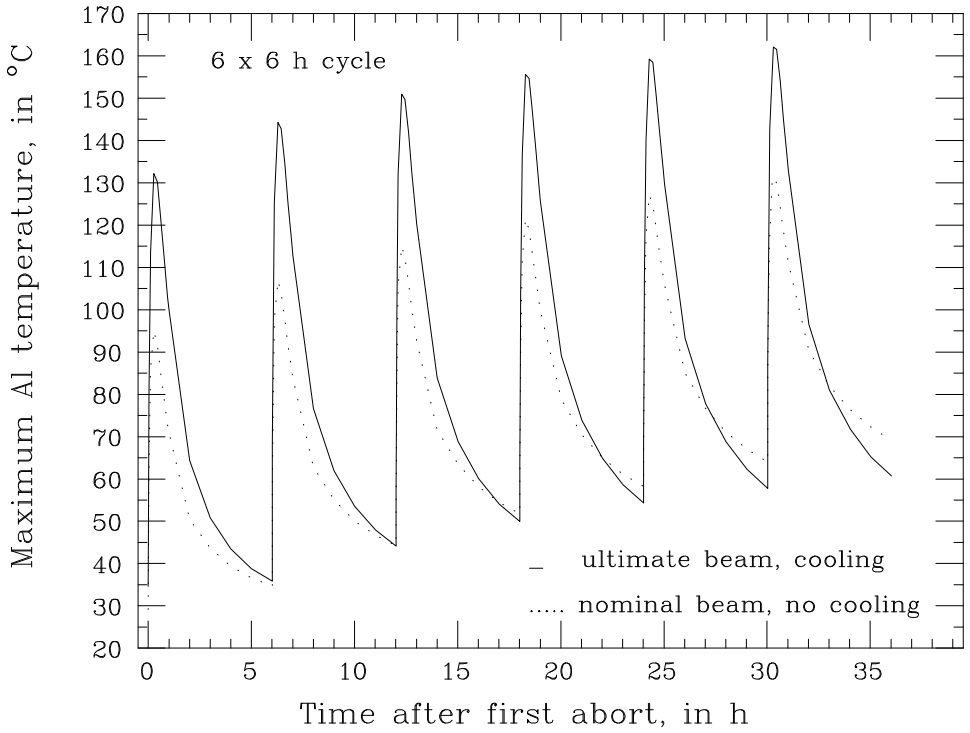

Figure 10c: Time evolution of the maximum temperature in the aluminium, over the first 6 thermal cycles of 6 h, for nominal (no cooling) and ultimate (water cooling) beam intensity.

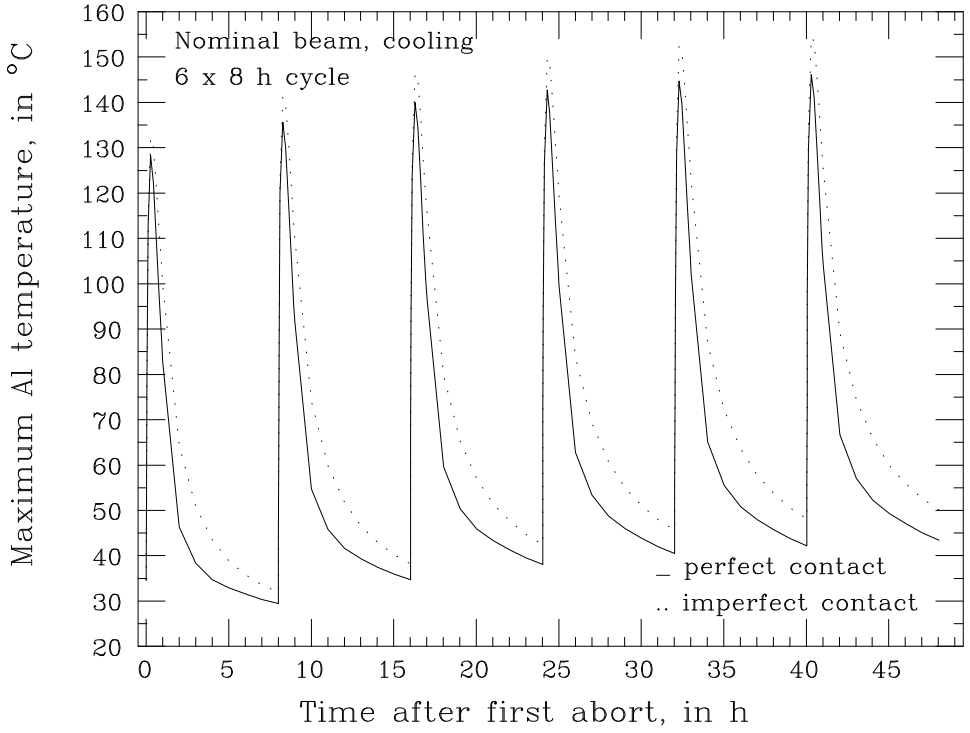

Figure 10d: Time evolution of the maximum temperature in the aluminium, over the first 6 thermal cycles of 8 h, for perfect and imperfect contact (water cooling, ultimate intensity).

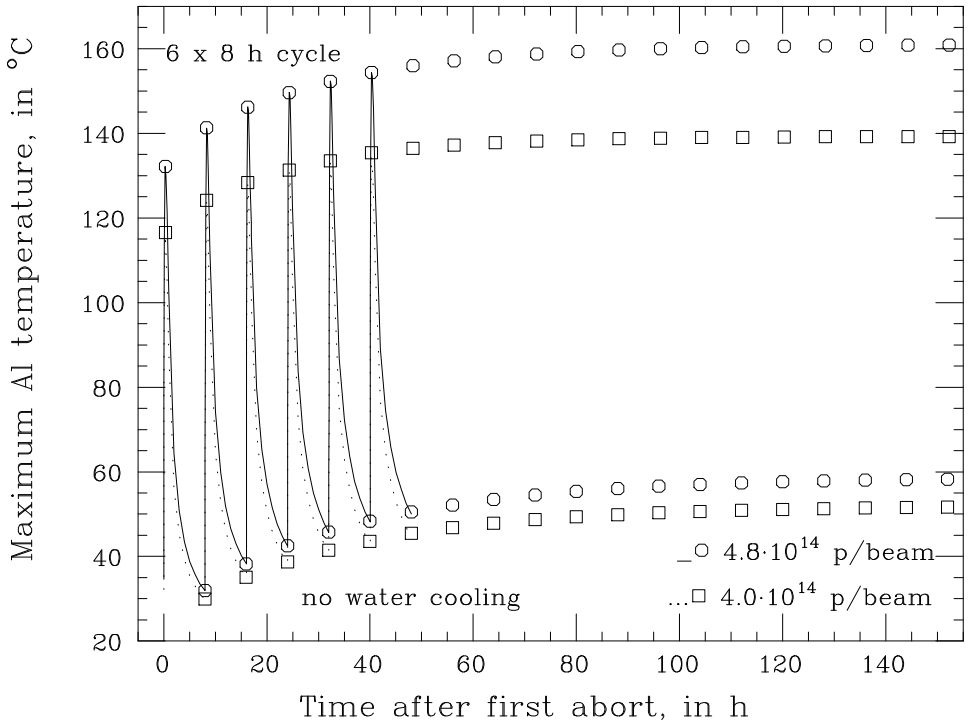

Figure 11: Comparison of the numerical approximation (see Section 6) to the ANSYS solution.

Table 6: Maximum and final temperatures [^{o}C] in the graphite core and Al frame, in the 6-th of subsequent beam abort cycles, for various cycle durations, beam intensities and cooling conditions. Extreme steady state temperatures in the Al frame are also included.

Cycle	Bunch	Water	Thermal	Maximum		Final		Steady in Al	
duration	intensity	cooling	contact	in C	in Al	in C	in Al	T_{min}	T_{Max}
1 h	ultimate	yes	poor	1327	297	317	250	332	371
1 h	ultimate	no	poor	1354	335	346	305	455	499
1 h	nominal	yes	poor	894	199	201	159	200	229
1 h	nominal	no	poor	911	221	219	193	307	319
3 h	ultimate	yes	poor	1246	194	118	112	126	214
3 h	ultimate	no	poor	1265	227	158	147	228	281
3 h	nominal	yes	poor	851	133	81	76	82	138
3 h	nominal	no	poor	860	154	103	97	150	192
6 h	ultimate	yes	poor	1225	162	77	68	72	171
6 h	nominal	no	poor	844	131	72	70	112	141
8 h	ultimate	yes	poor	1221	154	65	56	59	161
8 h	ultimate	yes	perfect	1218	146	53	51	55	150
8 h	4·1014 p	yes	poor	1053	135	57	50	52	139

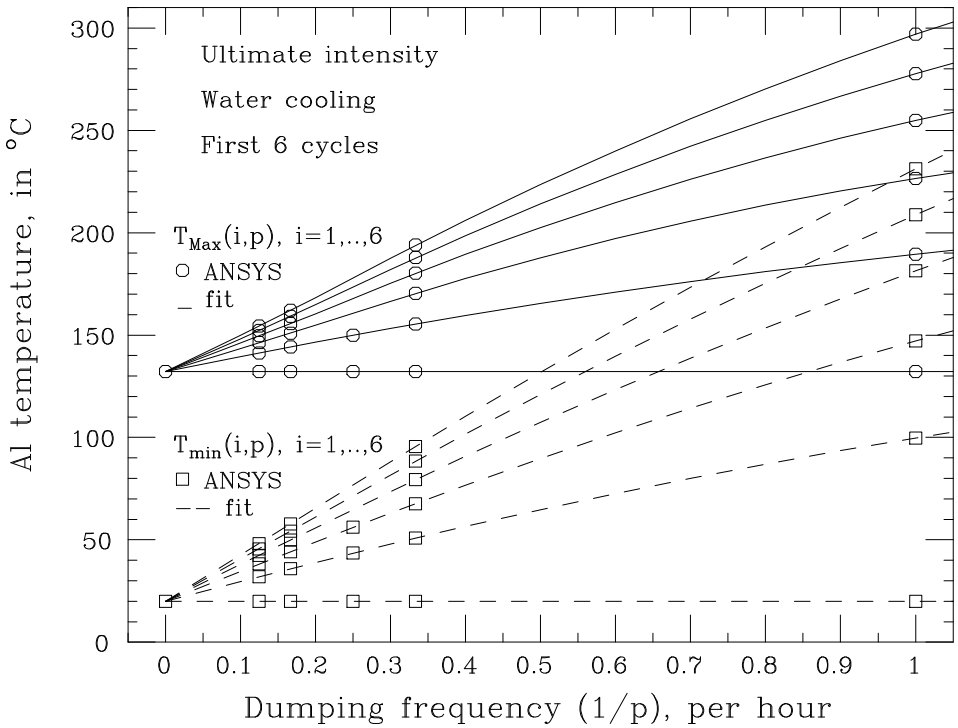

Figure 12a: Maximum and minimum temperatures in the Al frame over the first 6 cooling cycles, versus dumping frequency on water cooled dump, at ultimate intensity.

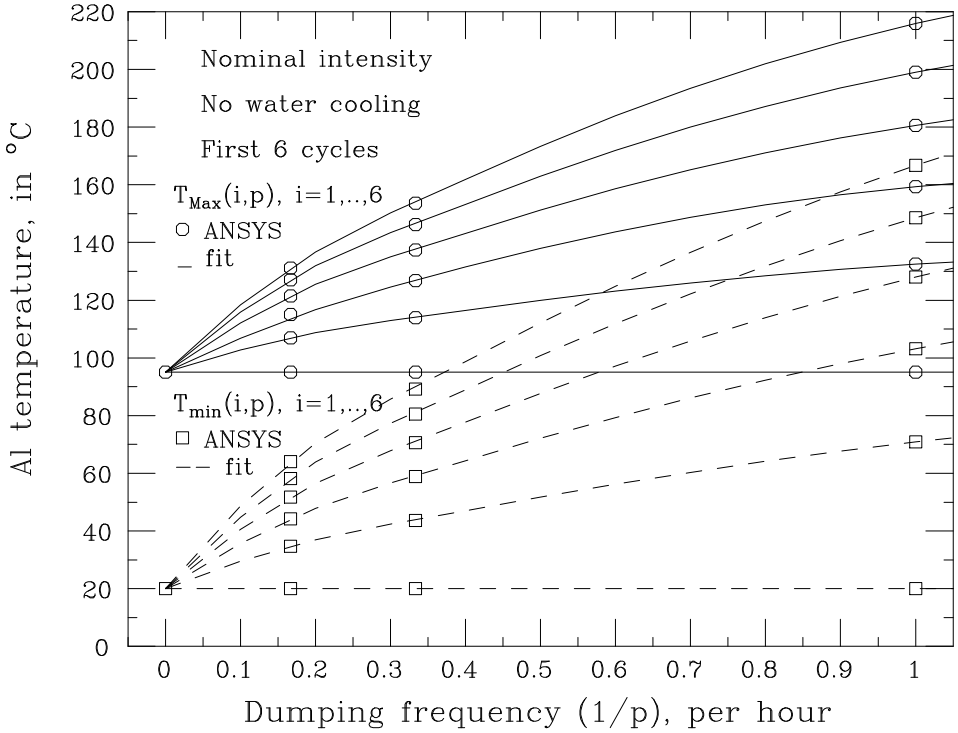

Figure 12b: Maximum and minimum temperatures in the Al frame over the first 6 cooling cycles, versus dumping frequency, without water cooling, at nominal intensity.

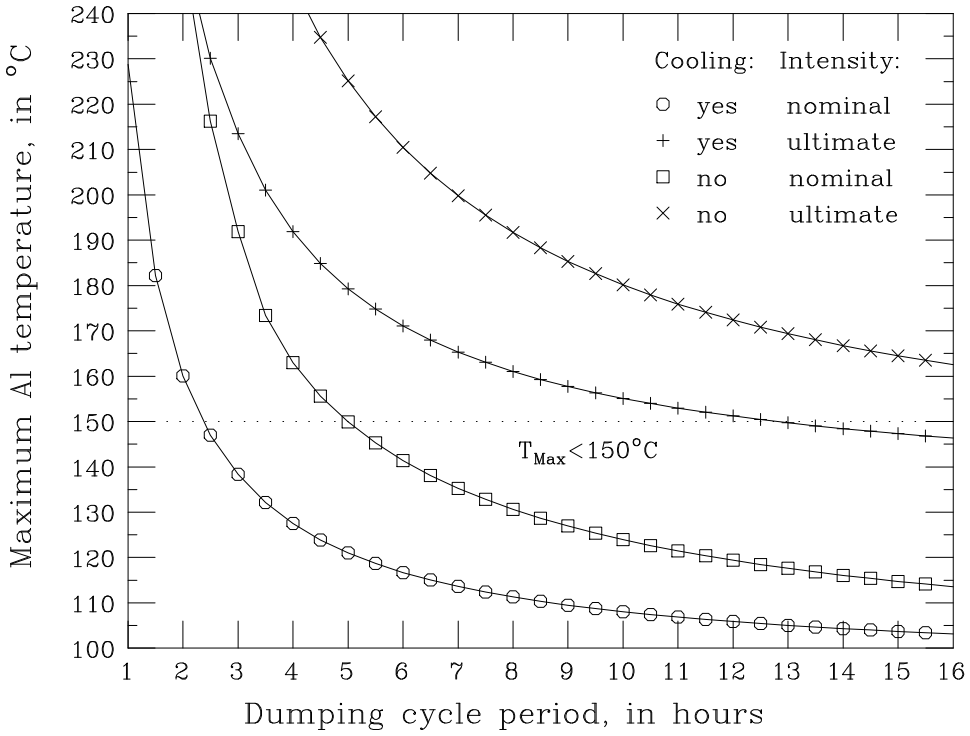

Figure 13: Stationary limit of the maximum temperature in the Al frame, as a function of dumping period, for nominal and ultimate beam intensity, with and without cooling.

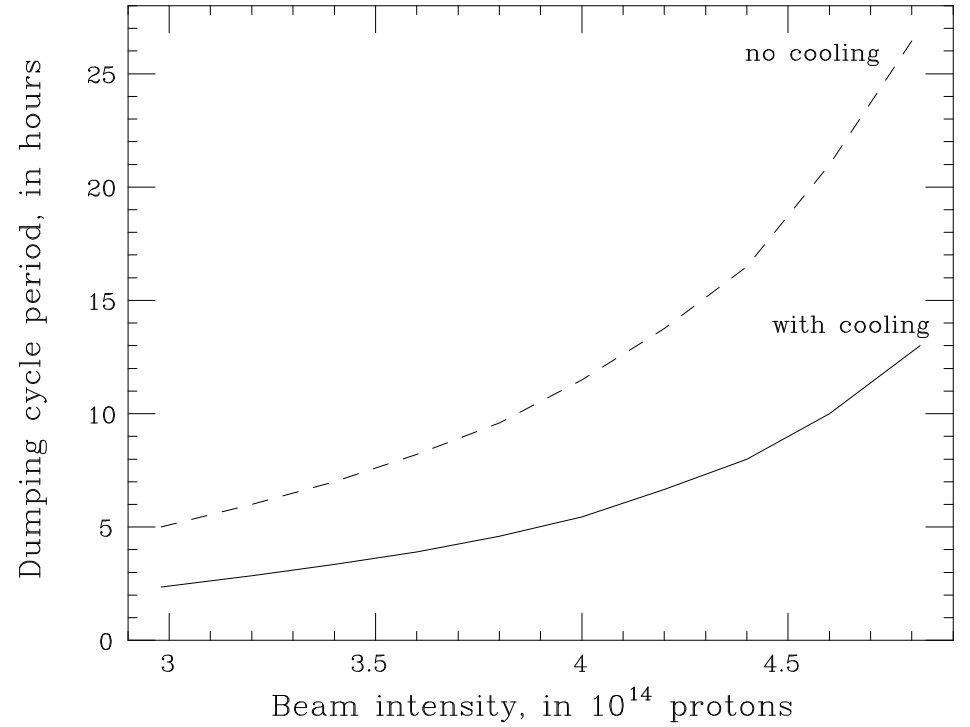

Figure 14: Minimum safe period (T_{Max} =150°C in Al frame) of repetitive aborts, as a function of beam intensity, with and without water cooling.